

Effect of Reactivity on Cure and Phase Separation Behavior in Epoxy Resin Modified with Thermoplastic Polymer: A Monte Carlo Simulation Approach

Won Ho Jo* and Moon Bae Ko

Department of Fiber and Polymer Science, Seoul National University, Seoul 151-742, Korea

Received November 5, 1993; Revised Manuscript Received September 8, 1994*

ABSTRACT: Structure development during the cure of epoxy resin modified with rubber or thermoplastic polymer was investigated by a Monte Carlo simulation technique. The lattice model of bond-fluctuation algorithm proposed by Carmesin and Kremer was modified to be applied to the crosslinking reaction between epoxy resin and curing agent. The entropy driven phase separation behavior was monitored by a quantity of collective structure factor and was analyzed by the Flory–Huggins theory. Even though the phase separation behavior near the critical composition of the mixture shows the spinodal decomposition irrespective of the cure rate, the phase separation mechanism at the off-critical composition is changed with the cure rate. The cure behavior seems to follow a second order reaction kinetics. As the volume fraction of added thermoplastic polymer increases, the apparent kinetic rate constant decreases at the same reactivity. This can be interpreted as a diluent effect of the added thermoplastic polymer on the cure kinetics. Also, the gelation behavior was compared with the Flory–Stockmayer branching theory.

Introduction

Thermoset epoxy resins are generally known to be brittle. Hence, the utilization of epoxy as a neat resin is not practical in many industrial applications. The incorporation of a second phase of dispersed rubbery particles or thermoplastic polymers in epoxy resins can greatly increase their toughness without any significant loss of the other desirable engineering properties.^{1,2} When an epoxy resin is modified with a thermoplastic polymer, the mixture of an epoxy prepolymer and a thermoplastic polymer is homogeneous at the initial stage, but at a certain thermoset conversion the thermoplastic polymers begins to be phase separated from the epoxy-rich matrix. The morphology development continues until the thermoset matrix reaches a conversion close to the gel point or vitrifies if the glass transition takes place before gelation. The final morphology of the cured system depends on the competition between crosslinking reaction and phase separation during cure. Thus the understanding of reaction kinetics and phase separation dynamics is of crucial importance in order to achieve an optimum phase structure.

Since polymers are very complicated topological objects, computer simulations are often the best tool to obtain precise theoretical information on the proposed model or to estimate the qualitative decoupled informations. Especially, the Monte Carlo method is a powerful simulation technique to study nonequilibrium processes including a large scale relaxation like the cure process of epoxy resins modified with thermoplastic polymers. Even though many lattice algorithms that obey Rouse dynamics are also given in the literatures,^{3–6} these algorithms have the drawback that the relaxation of branched structures cannot be achieved using these algorithms. However, Carmesin and Kremer⁷ proposed a bond fluctuation algorithm and simulated the dynamics of branched polymer.

In our previous paper,⁸ we applied this bond fluctuation algorithm for the simulation of structure development on a cubic lattice when an epoxy prepolymer is cured with a crosslinking agent in the presence of

thermoplastic polymer. The effects of the reactivity between an epoxide group and a crosslinking agent on the development of phase morphology were studied in terms of the growth of the collective structure factor. In the present study, the cure and gelation behavior as well as the structure development were investigated by a Monte Carlo technique when the reactivity between an epoxide group and a crosslinking agent was varied at various compositions of epoxy and thermoplastic polymers, and then the results were systematically analyzed upon the basis of the Flory–Stockmayer branching theory and the Flory–Huggins theory.

Model and Simulation Technique

In this study, the two-dimensional bond fluctuation model proposed by Carmesin and Kremer⁷ for the dynamics of linear and/or crosslinked chains was extended to a three-dimensional one on a simple cubic lattice (SC) as described in our previous paper.⁸ Each segment of thermoplastic or epoxy prepolymer occupies eight sites of a unit cell. For convenience, it is assumed that an uncured epoxy prepolymer corresponds to one Kuhn segment and thus occupies eight sites of a SC lattice. A thermoplastic polymer is depicted as one comprised of five effective units referred to the volume of an epoxy prepolymer upon the construction of a coarse-grained model for a linear polymer. In this model the bond length l , i.e., the distance between two linked segments, is not fixed. The minimum value for any l is 2 lattice units (lu), and the maximum is $10^{1/2}$ lu. In between, the bond length l can have values such as $5^{1/2}$, $6^{1/2}$, and 3 lu. This condition automatically ensures that bond vector cannot intersect, and hence entanglement restrictions can be taken into account in a very simple manner.⁹ A randomly selected segment may move the distance of one lattice unit into one of six SC lattice directions subjected to four conditions: the self- and mutually avoiding walk condition, the bond length restriction, energetical transition criterion and no bond crossing.

One more criterion, i.e., the Metropolis transition probability as an energetical criterion, is also used. The configurational energy change ΔE between before and after each move is appropriately taken into account with

* Abstract published in *Advance ACS Abstracts*, November 15, 1994.

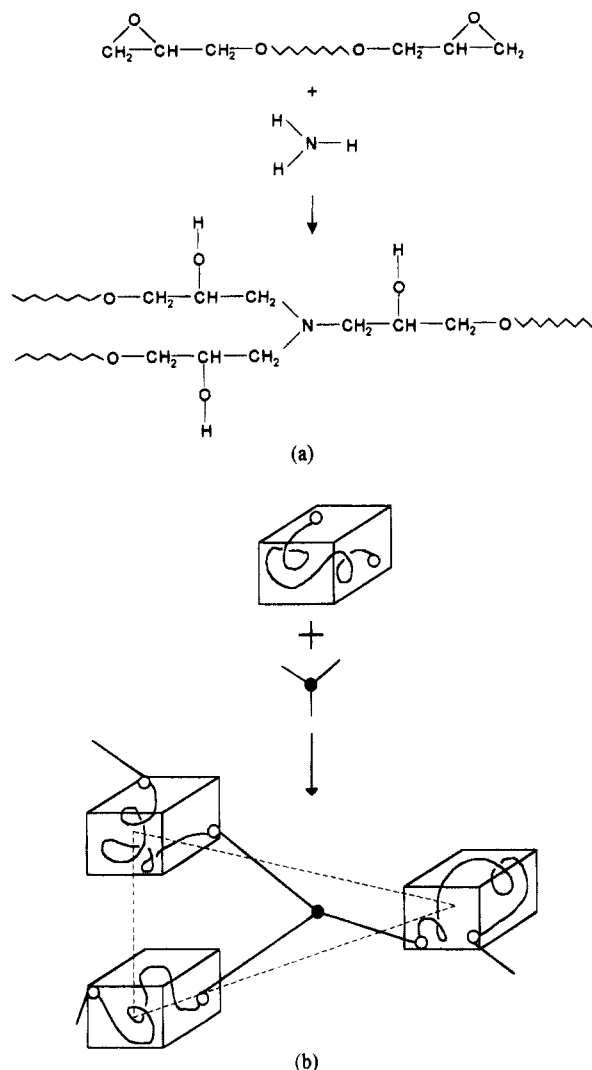


Figure 1. Schematic reaction of difunctional epoxy prepolymer and trifunctional amine (a) and its coarse-grained modeling on eight site bond fluctuation algorithm (b). The solid curve in a cube represents the bifunctional epoxy prepolymer. The markers \circ and \bullet denote epoxide group of epoxy prepolymer and crosslinking agent, respectively.

a transition probability $W = \min\{1, \exp(-\Delta E/kT)\}$. The unit ϵ is defined as the magnitude of the repulsive interaction energy per segment between epoxy prepolymer and thermoplastic polymer, irrespective of the distance between two as long as the distance is smaller than $6^{1/2}$ lu. The interaction energies between the same molecules are assumed to be zero. The time unit, a Monte Carlo step (mcs), is defined as one attempted trial per statistical segment of epoxy prepolymer or thermoplastic polymer on the average. Because we randomly choose the lattice site for attempted move, L^3 trials for choosing the lattice site correspond to 8 mcs.

Figure 1 depicts the reaction of epoxide group and amine (a) and its modeling on eight sites bond fluctuation algorithm (b). In this model a crosslinking agent occupies one lattice site, while an epoxy prepolymer occupies eight lattice sites. The completely reacted triamine has three bonds with nearest epoxy prepolymers. These real bonds are depicted by solid lines in Figure 1b. However, we checked the imaginary bonds (the dashed lines in Figure 1b) between nearest epoxy prepolymers linked with the same crosslinking agent under bond length restriction when the epoxy polymer moves. If a randomly chosen lattice site is occupied by a crosslinking agent, three types of motions may be

considered. First, suppose that a randomly chosen crosslinking agent is in contact with a part of epoxy prepolymer segment which occupies one of six nearest coordinates of a crosslinking agent. The reaction probability p is assumed to be equal to the product of the reactivity r , the number of unreacted functional groups of the chosen crosslinking agent, and the unreacted probability of epoxide that the selected nearest site, being a part of epoxy prepolymer, has an unreacted epoxide functional group. The unreacted probability of epoxide corresponds to the value of the number of unreacted epoxide groups in randomly selected nearest epoxy prepolymer divided by eight. If p exceeds a random number between 0 and 1, the reaction between the functional group of crosslinking agent and the epoxide group is allowed. For simplicity, it is assumed that any intramolecular reaction in the same epoxy prepolymer cannot occur. Secondly, if a randomly selected lattice site of six nearest coordinates around the crosslinking agent is an empty void, the chosen crosslinking agent moves into this empty void. However, if the chosen crosslinking agent is bonded by at least one epoxy prepolymer, it moves into this empty void with the constraint that the bonds could not deviate above the length of three lattice units from all epoxy prepolymer segments linked to this crosslinking agent. This motion ensures that crosslinking agents are distributed homogeneously through the mixture. Thirdly, if a randomly chosen lattice site of six nearest coordinates around a crosslinking agent is occupied by inert thermoplastic polymer, no motion takes place.

Collective Structure Factor. In order to investigate the time evolution of the long range ordering, it is very convenient to compute the collective structure factor of the system. For the binary mixture, the starting point of the description is a Flory-Huggins lattice model of the polymer mixture, where a local concentration variable ϕ_P^j is equal to 1 if lattice site j is taken by a thermoplastic polymer segment and otherwise zero, and ϕ_E^j is equal to 1 if it is taken by an epoxy prepolymer segment and otherwise zero. Then the time dependent collective structure factor of an $L \times L \times L$ lattice, with L being equal to 45 and periodic boundary conditions applied, is given by^{10,11}

$$S(\mathbf{q}, t) = \left\langle \sum_{\mathbf{r}_i} \sum_{\mathbf{r}_j} \exp(i\mathbf{q} \cdot \mathbf{r}_{ij}) (\xi^i \xi^j - \langle \xi \rangle^2) \right\rangle / L^3 \quad (1)$$

where $\langle \rangle$ denotes a thermal statistical average, ξ^j represents $(\phi_P^j - \phi_E^j)$, and \mathbf{r}_{ij} is the vector between the lattice sites i and j . The sum runs over the lattice, and vector \mathbf{q} is selected as $\mathbf{q} = (2\pi/L\Delta r)\mathbf{n}$, in which \mathbf{n} represents positive integer vector, e.g., $\mathbf{n} = (0, 1, 2)$, $(1, 2, 3)$, $(1, 1, 2)$, etc. This quantity represents the Fourier transform of the pair-correlation function. We then define a spherically averaged structure factor as eq 2

$$S(q, t) = \sum_{q - (\Delta q/2) \leq q \leq q + (\Delta q/2)} S(\mathbf{q}, t) / p(\mathbf{q}, \Delta q) \quad (2)$$

where

$$p(\mathbf{q}, \Delta q) = \sum_{q - (\Delta q/2) \leq q \leq q + (\Delta q/2)} 1 \quad (3)$$

The quantity defined in eq 3 denotes the number of lattice points in a spherical shell of radius q with Δq in shell thickness. Ideally, one must take Δq as small as

Table 1. Calculation of the Parameters for Various Epoxy Formulations

	sample		
	A	B	C
ϕ_P	0.289	0.177	0.058
ϕ_E	0.311	0.414	0.525
ϕ_C	0.026	0.035	0.044
$\bar{\phi}_P$	0.481	0.300	0.100
$\bar{\chi}$	0.600	0.591	0.584
ϕ_2	0.462	0.283	0.093
χ'^a	0.603	0.612	0.623

^a Average $\chi' = 0.613$.

possible. To save the computing time for $S(q,t)$, Δr is selected as 3 and hence $\Delta q = (2\pi/3L)$.

Results and Discussion

Cure Kinetics. Since the cure model presented in the section of Model and Simulation Technique is expected to describe a time-dependent behavior, it is necessary to clarify what the time is in this model. Let us set $t = 0$ for the time when the growth begins. The time unit, a Monte Carlo step (mcs), is defined as one attempted trial per statistical segment on the average. Then the time t is equal to the number of trials for move of a respective segment. When there are molecules of different sizes, the definition of the Monte Carlo time scale can be rather subtle. But, the lattice sites are randomly chosen in this study, thus, L^3 trials for choosing the lattice site correspond to 8 mcs. Note that a respective crosslinking agent attempts to react or to move one time for 8 mcs regardless of the success of the reaction. In a strict sense, this definition of a time unit is arbitrary, but it is believed that it coincides more or less with reality. This will be confirmed first by the cure behavior of all stoichiometric mixtures of epoxy and crosslinking agent at various compositions of epoxy prepolymer and thermoplastic polymer. The sample formulations are listed in Table 1, in which ϕ_P , ϕ_E , and ϕ_C indicate the number fractions of lattice sites occupied by thermoplastic polymer, epoxy prepolymer, and crosslinking agent, respectively.

The degree of cure α is defined as the ratio of the number of reacted epoxide groups, N_t , to the total number of epoxide groups in the system, N_0 :

$$\alpha = N_t/N_0 \quad (4)$$

Figure 2a is the plots of the degree of cure as a function of curing time. As expected, the figure shows that the degree of cure α rises rapidly at the initial stage of cure. No induction time is observed in any case, irrespective of the reactivity r and the formulation of the mixture. A common feature of many epoxy resin systems is that the curing mechanism is autocatalytic in nature. If this mechanism is involved, the plot of the degree of cure *vs* curing time shows the sigmoidal shape. Many researchers^{12,13} investigated the cause of the sigmoidal shape, suggesting the presence of more than one type of kinetic mechanism, e.g., the mechanism in which the hydroxyl group *in situ* formed as a result of the reaction between the primary amine and epoxide group catalyze the reaction between the secondary amine and an epoxide. However, the simulation shows no induction period, indicating a simple n th-order reaction. Thus, the cure rate is assumed to follow a n th-order kinetics:¹⁴⁻¹⁶

$$\frac{d\alpha}{dt} = K(1-\alpha)^n \quad (5)$$

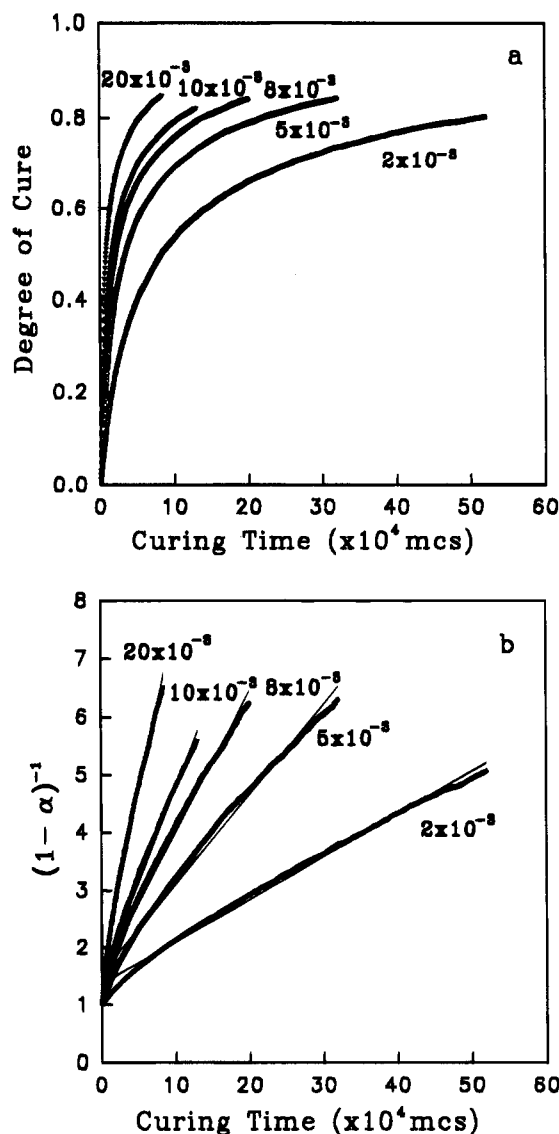


Figure 2. (a) Plot of degree of cure α *vs* curing time t . (b) Plot of $(1 - \alpha)^{-1}$ *vs* curing time t for sample B. The values in the legend represent the reactivities and the characteristics of samples are listed in Table 1.

where K is a kinetic rate constant. The probability that randomly chosen crosslinking agent may react with epoxy prepolymer is proportional to the product of the number of unreacted functional groups pertaining to the crosslinking agent and the probability that the chosen nearest site of epoxy prepolymer is occupied by an unreacted epoxide group. These two quantities are proportional to $(1 - \alpha)$; thus, it may be assumed that the crosslinking reaction follows a second order reaction. When the reaction is assumed second order, i.e., $n = 2$, eq 5 is written as eq 6:

$$\frac{1}{1-\alpha} = Kt + 1 \quad (6)$$

By plotting $(1 - \alpha)^{-1}$ against curing time t , the apparent rate constant K can be calculated from the slope of the plot in Figure 2b if the reaction obeys the second-order kinetics. However, the plots of Figure 2b are slightly curved. This is probably due to the model used, with excluded volume and chain connectivity but intramolecular reactions prohibited. It is noteworthy that the plots of $-\ln(1 - \alpha)$ *versus* Kt , when the reaction is assumed a first order reaction, are more curved than the ones for the second order kinetics. Figure 2b shows

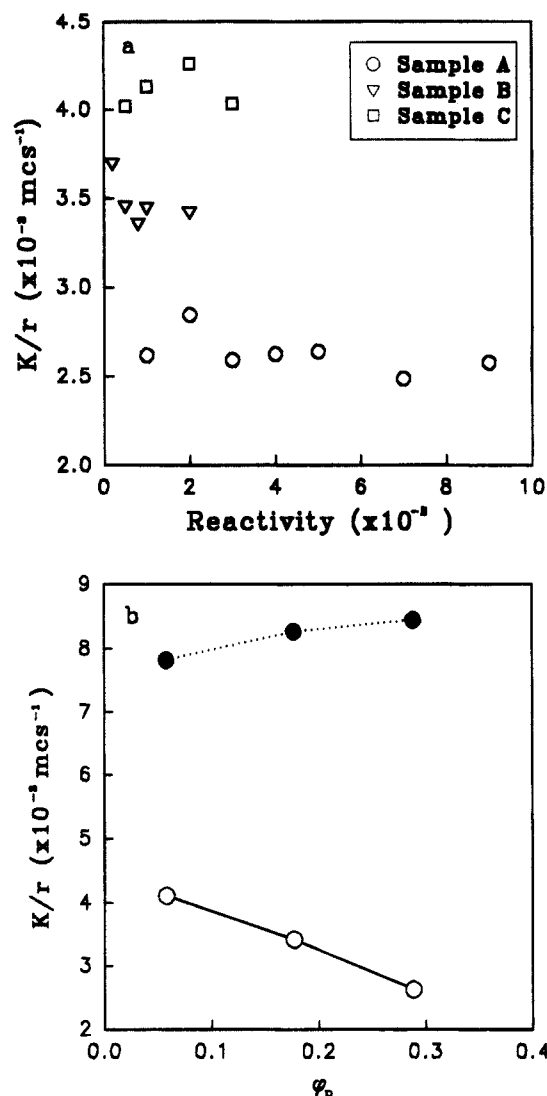


Figure 3. (a) Plot of the reduced kinetic constant (K/r) vs reactivity r . (b) Plot of K/r vs ϕ_E , which is represented by the symbol ○. In b, The symbol ● represents the (K/r) normalized with respect to the volume fraction of epoxy prepolymer, ϕ_E .

that the kinetic rate constant K increases with the reactivity r .

However, as seen in Figure 3a, when the kinetic rate constant is normalized with respect to the reactivity r , the normalized kinetic rate constant (K/r) is almost independent of r . Since the reactivity r is introduced in our modeling as the probability that the crosslinking agent reacts with the selected nearest epoxide group, the overall kinetic rate constant K should be directly proportional to the reactivity r . As the volume fraction of thermoplastic polymer increases, the average value of K/r in Figure 3a decreases. Generally, the kinetic rate constant K is described by the Arrhenius equation

$$K = A_T \exp(-E/kT) \quad (7)$$

where A_T is a pre-exponential factor and E is an activation energy for crosslinking reaction between epoxy and crosslinking agent. For the reaction kinetics controlled by the segment motion, the pre-exponential factor A_T can often be expressed as a WLF form. In the presence of thermoplastic polymer, it is expected that frequency factor A_T of the reaction between epoxy and curing agent becomes lower. Thus the reaction becomes slower as the volume fraction of thermoplastic polymer increases. A certain selected curing agent happens to

react with epoxy prepolymer only if the condition, that a randomly selected nearest neighbor of six coordinates is occupied with epoxy prepolymer, is satisfied. The probability that the randomly selected lattice site is occupied with epoxy prepolymer is proportional to the volume fraction of epoxy prepolymer, ϕ_E , in Table 1. Thus, the quantity (K/r) may be normalized with respect to ϕ_E , as shown in Figure 3b. Contrary to expectations, however, the result shows that the normalized value slightly increases with the volume fraction of thermoplastic polymer.

An effective self-diffusion coefficient of the chains (i.e., epoxy prepolymer and thermoplastic polymer) can be calculated from eq 8¹⁷

$$D_{eff}^{EP}(t, \Delta t) = \frac{\langle [r_{CG}(t) - r_{CG}(t - \Delta t)]^2 \rangle_{EP}}{6\Delta t} \quad (8)$$

where $r_{CG}(t)$ is the center of gravity of an epoxy prepolymer or a thermoplastic polymer at a given time t from the beginning of cure, and the average in eq 8 is taken over all polymers of epoxy prepolymer and thermoplastic polymer. The time interval, Δt , in eq 8 should, in principle, be greater than the chain relaxation time. But it was limited rather to $\Delta t = 400$ mcs for practical reasons. The calculated diffusion coefficient of an epoxy polymer in the system of larger volume fraction of thermoplastic polymer is greater than that of smaller volume fraction of thermoplastic polymer. Thus, the result in Figure 3b comes from the fact that the diffusion coefficient of an epoxy polymer increases with the volume fraction of thermoplastic polymer.

Gelation Behavior. In this study, a method, named the "cluster multiple labeling technique",¹⁸ suitable for computer simulation and applicable for a fast and accurate determination of cluster distribution, was used. More pronounced effects at the gel point are shown by the weight-average cluster size defined as eq 9

$$DP_W = \sum_{s=1}^{\infty} s^2 n_s / \sum_{s=1}^{\infty} s n_s$$

$$RDP_W = \sum_{s=1}^{\infty} s^2 n_s' / \sum_{s=1}^{\infty} s n_s' \quad (9)$$

where s and n_s represent the size and the number of cluster of size s , respectively and the prime means that the largest cluster is omitted from the summation. The reduced weight-average cluster size, RDP_W , is plotted against curing time in Figure 4a. All curves show the maximum, where the time is often defined as a gelation time. Since the largest cluster is omitted in the calculation of RDP_W , RDP_W increases with curing time (or degree of cure) and then abruptly falls down after the largest cluster and the second coalesce into a single large cluster. Figure 4b is the plot of RDP_W against degree of cure α , showing that all curves fall into a single curve. Various methods have been previously used to determine a gel point: (1) the maximum slope of the modified second moment of the cluster distribution,¹⁹ (2) the maximum reduced average cluster size,¹⁸ and (3) log-log plots of DP_W vs degree of cure.²⁰ Since RDP_W reaches a maximum whenever there are two or more large clusters, it often gives a lower bound to the true gel point. In this study, the degree of cure at which RDP_W shows a maximum peak is taken to be the gel

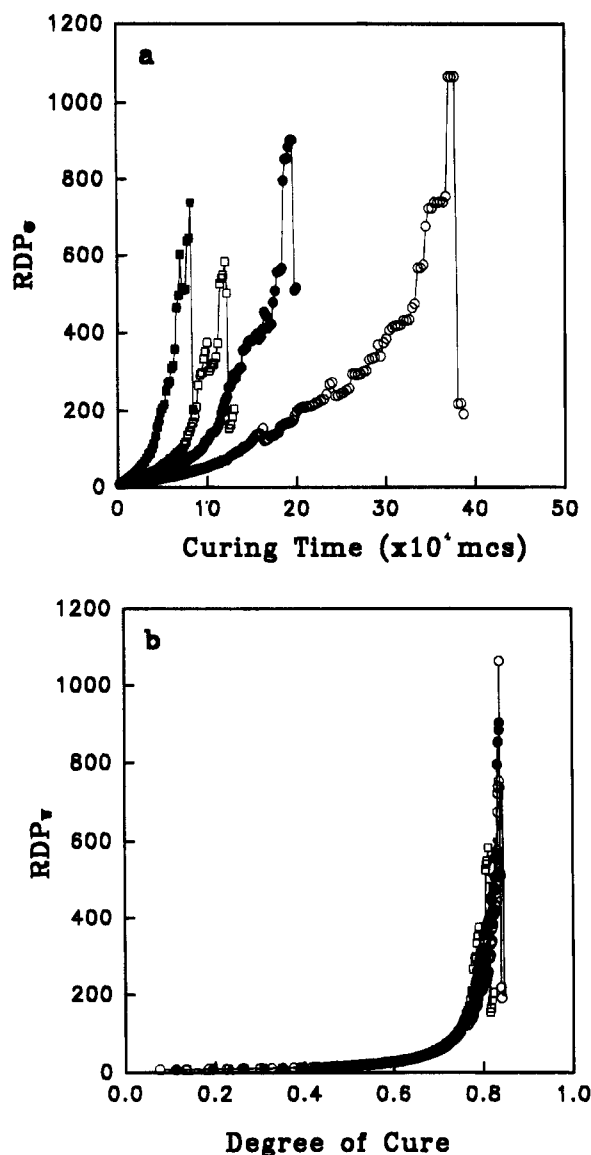


Figure 4. Plots of reduced average cluster size, RDP_w , against (a) curing time or (b) degree of cure: ■, $r = 20 \times 10^{-3}$; □, $r = 10 \times 10^{-3}$; ●, $r = 8 \times 10^{-3}$; ○, $r = 5 \times 10^{-3}$.

point, α_g . All gel points determined from the peak points in Figure 4b were averaged, and the mean value is 0.837.

Let $\bar{V}_{1,0}$ be the initial molar volume of the epoxy-curing agent mixture defined as eq 10

$$\bar{V}_{1,0} = \frac{A_3 \bar{V}_{A_3} + B_2 \bar{V}_{B_2}}{A_3 + B_2} \quad (10)$$

where A_3 and B_2 represent the number of moles of both components, i.e., trifunctional curing agent and bifunctional epoxy prepolymer, respectively. For a stoichiometric mixture of these components, i.e., $2B_2 = 3A_3$, eq 10 reduces to

$$\bar{V}_{1,0} = \frac{\bar{V}_{A_3} + (3/2)\bar{V}_{B_2}}{5/2} \quad (11)$$

Thus, the value of $\bar{V}_{1,0}$ for our model is equal to 5.2 (lu^3). If z_1 is the ratio of molar volume of epoxy polymer to $\bar{V}_{1,0}$, z_1 increases with degree of cure. Then

$$z_1 = \frac{\bar{V}_1}{\bar{V}_{1,0}} = \frac{A_3 + B_2}{N} \quad (12)$$

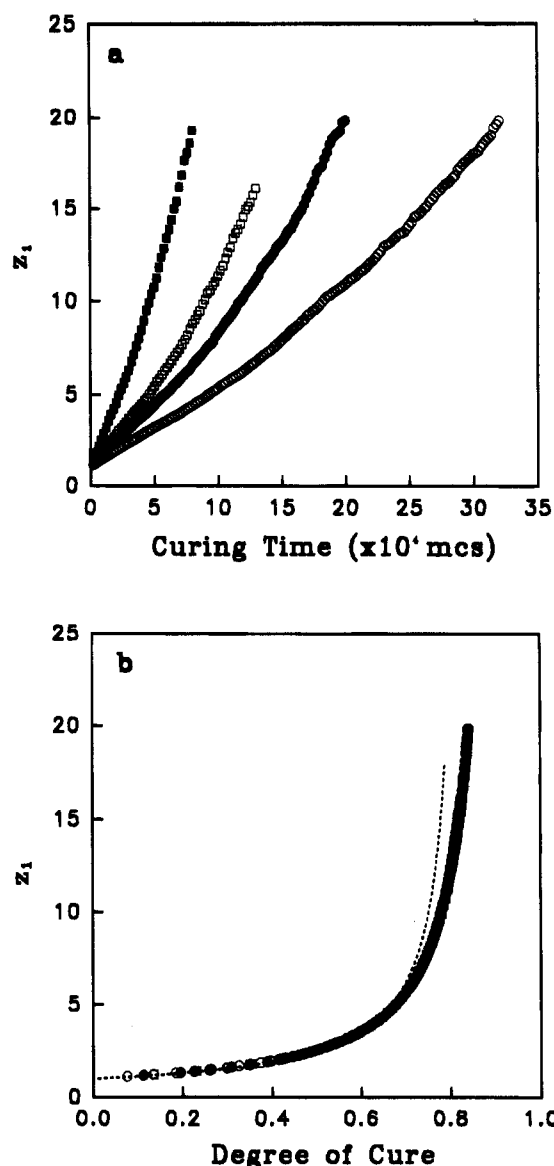


Figure 5. Plots of z_1 against (a) curing time or (b) degree of cure: ■, $r = 20 \times 10^{-3}$; □, $r = 10 \times 10^{-3}$; ●, $r = 8 \times 10^{-3}$; ○, $r = 5 \times 10^{-3}$.

where N is the total number of clusters. According to the classical Flory-Stockmayer theory,²¹ the total number of clusters, N , is given by

$$N = A_3 \left(\frac{5}{2} - 3\alpha \right) \quad (13)$$

for a stoichiometric mixture of trifunctional curing agent and bifunctional epoxy prepolymer. Then z_1 in eq 12 reduces to

$$z_1 = \left(1 - \frac{6}{5}\alpha \right)^{-1} \quad (14)$$

Thus, the gel point is calculated when z_1 is infinite. The value of $\alpha_g = 0.837$ obtained from our simulation is nearly consistent with the value of $\alpha_g = 0.833$ predicted by Flory and Stockmayer, although it has been known that there are severe finite size effects and strong effects of fluctuation in computer simulation.

Figure 5a is a plot of z_1 versus curing time at various reactivities. The figure shows that z_1 increases much more rapidly with increasing reactivity. Figure 5b is a plot of z_1 versus degree of cure α , showing that all curves fall on a single curve irrespective of reactivity. The

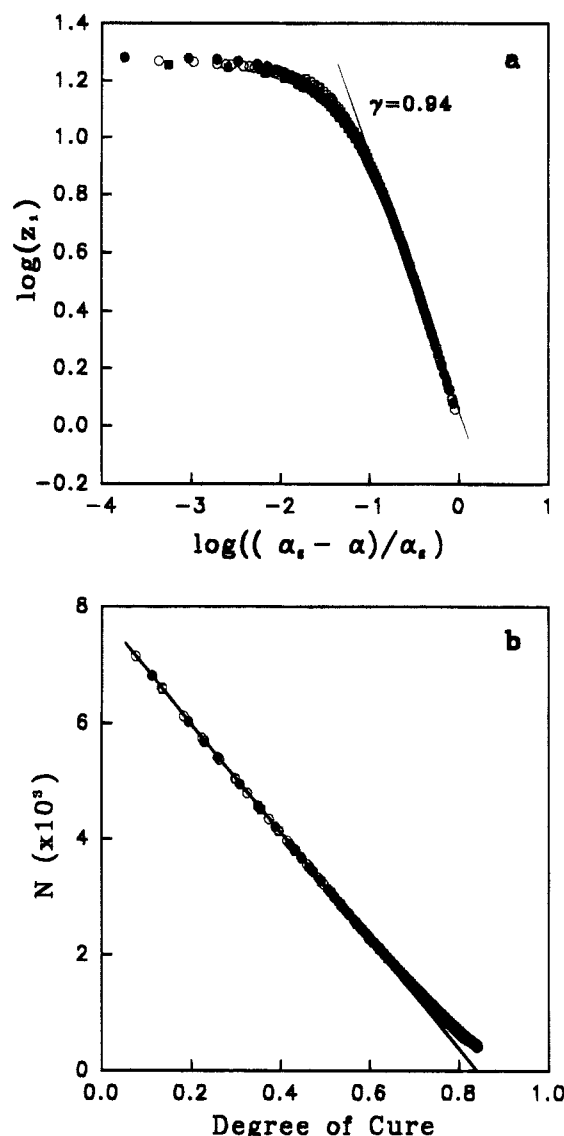


Figure 6. Comparison of simulation data with the Flory-Stockmayer theory: ■, $r = 20 \times 10^{-3}$; □, $r = 10 \times 10^{-3}$; ●, $r = 8 \times 10^{-3}$; ○, $r = 5 \times 10^{-3}$.

dashed line represents the plot of z_1 versus degree of cure, according to eq 14. In the range of low degree of cure, the simulation result is fitted well to eq 14, but some deviation from eq 14 is observed in the region of high degree of cure.

For the pregel region, i.e., below α_g , the following relationship may be constructed

$$z_1 = C(\alpha_g - \alpha)^{-\gamma} \text{ for } \alpha \rightarrow \alpha_g \quad (15)$$

where C is the critical amplitude in pregel region. Figure 6a is a log-log plot of z_1 versus $|\alpha - \alpha_g|/\alpha_g$, in which the simulation value of 0.837 was used for α_g , showing that the linearity between $\log(z_1)$ and $\log(|\alpha - \alpha_g|/\alpha_g)$ is held while strong deviation is found in the region of high degree of cure. The value for γ in eq 15 was estimated to be 0.94 by the best-fit to a straight line. The value 0.94 is nearly consistent with the value of the classical Flory-Stockmayer theory.²¹ Flory²¹ derived eq 14, assuming that intramolecular reaction does not occur between the same molecule. Although our cure model does not allow the formation of rings in the same epoxy prepolymer, the intramolecular reaction between different epoxy prepolymers pertaining to the same cluster might be allowed. If this happens, the

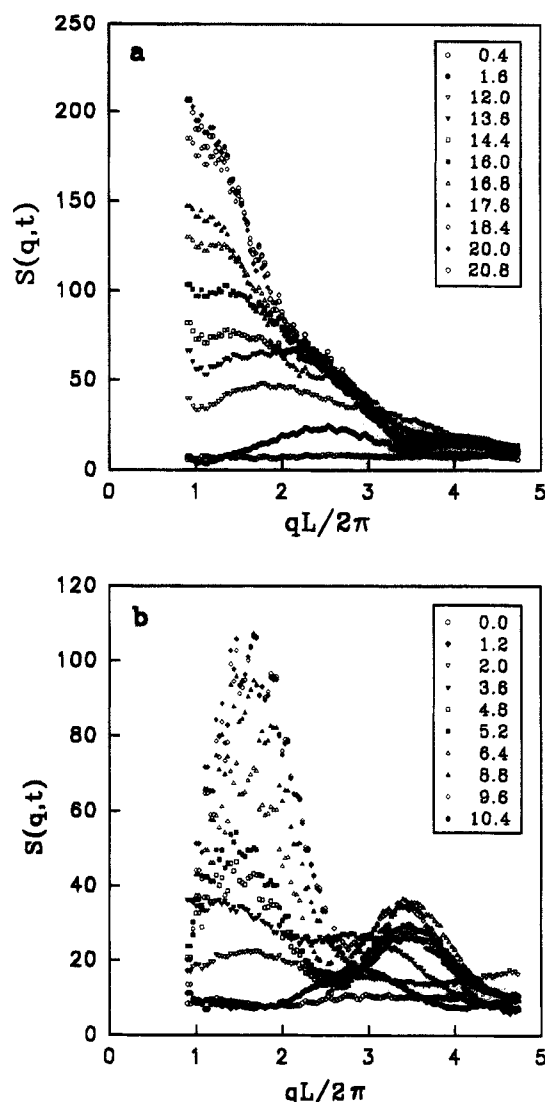


Figure 7. Time evolution of structure factor $S(q,t)$ plotted against the magnitude of scattering vector, q for sample A: (a) $r = 10 \times 10^{-3}$; (b) $r = 20 \times 10^{-3}$. The values in the legends indicate the curing times in unit of 10^4 mcs.

number of clusters is larger than that estimated by Flory, at the same degree of cure. This appears remarkably at the late stage of cure. Figure 6b shows the deviation of the number of clusters between the Flory and the simulation result. Apparently, Flory underestimated the number of clusters for a high degree of cure. However, the estimation of the number of clusters by Flory (see eq 13) seems to have a good agreement with the simulation result up to a degree of cure, ca. 0.65.

Structure Development during Cure. Figures 7 and 8 are some typical examples for the time evolution of structure factor $S(q,t)$ plotted against the magnitude of scattering vector, q . The figures show that the structure factor $S(q,t)$ increases with curing time, and then the growth is retarded and finally stopped after a certain time elapses. As a random mixture of thermoplastic polymer and epoxy prepolymer, which is initially structureless and homogeneous, is cured, the mixture starts to separate into epoxy rich phase and thermoplastic rich one. The number of hetero-pair contacts between epoxy segment and thermoplastic polymer decreases much rapidly as the cure rate increases (not shown here). This is caused by rapid phase demixing driven by the entropy loss due to the rapid increase in

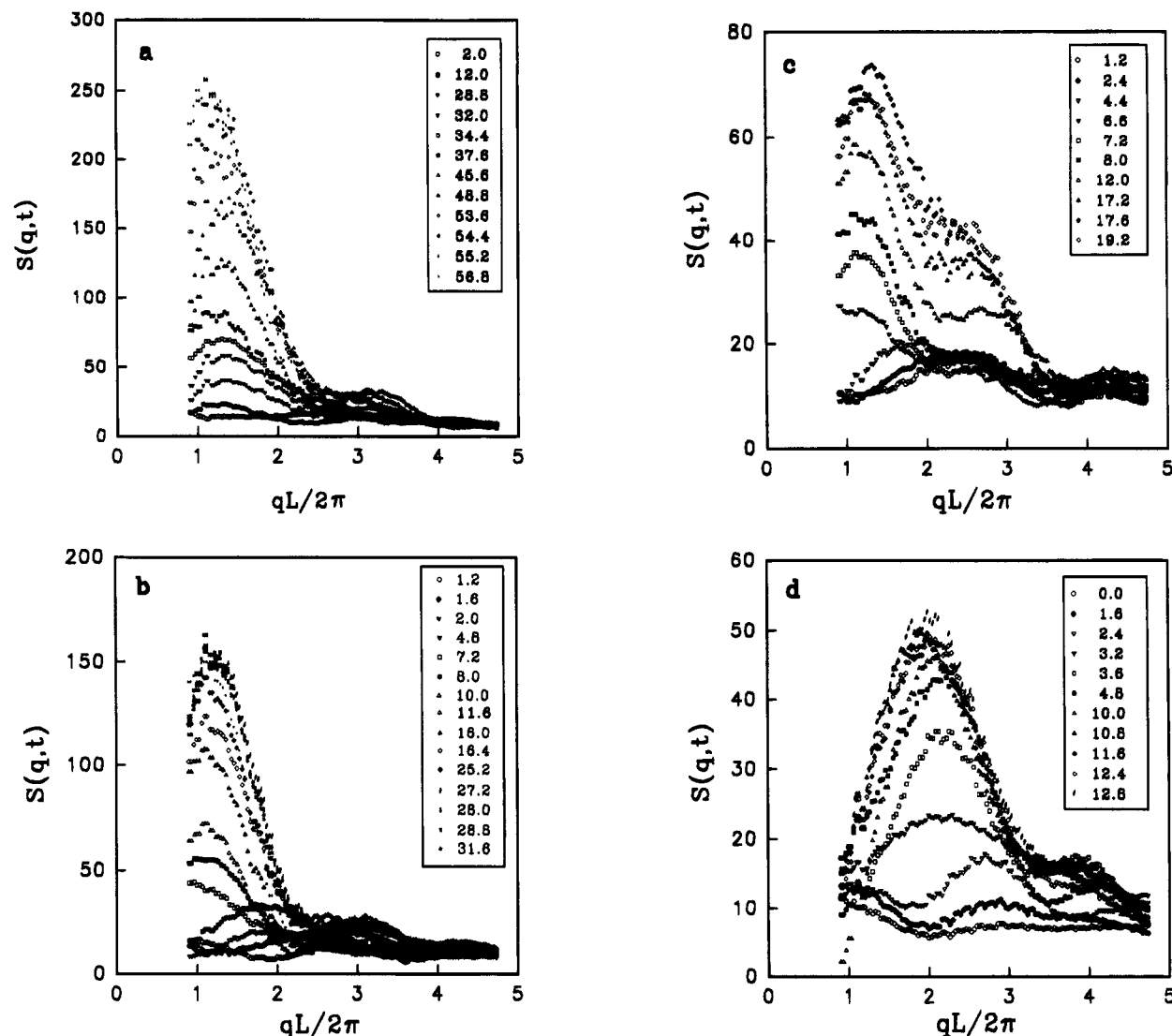


Figure 8. Time evolution of structure factor $S(q,t)$ plotted against the magnitude of scattering vector, q for sample B: (a) $r = 2 \times 10^{-3}$; (b) $r = 5 \times 10^{-3}$; (c) $r = 8 \times 10^{-3}$; (d) $r = 10 \times 10^{-3}$. The values in the legends indicate the curing times in unit of 10^4 mcs.

the molecular weight of epoxy resin as the cure proceeds.

Recently, Deutch and Binder⁹ related the repulsive interaction energy ϵ between pair of statistical segments to the Flory-Huggins interaction parameter χ in the eight site bond fluctuation algorithm. In using the Metropolis transition probability, only the interaction between the unlike segments which are at distance from 2 lu to $6^{1/2}$ lu is considered in the calculation of energy change, ΔE . Thus, the Flory-Huggins interaction parameter χ can be related to the repulsive interaction energy ϵ as eq 16

$$\chi = 14\epsilon/(kT) \quad (16)$$

where 14 is an effective coordination number, which is the maximum number of effective statistical segments that one statistical segment can interact with. Equation 16 is rigorously true for $\phi_v = 0$, where ϕ_v indicates the sum of volume fractions of the vacant sites and the sites occupied by crosslinking agents since a crosslinking agent and a vacancy have no interaction energy with any component in our simulation model. For $\phi_v \neq 0$, a simple generalization of the Flory-Huggins theory yields^{22,23}

$$\bar{\chi} = \chi(1 - \phi_v) = (14\epsilon/kT)(1 - \phi_v) \quad (17)$$

Thus, the enthalpy term of free energy of mixing can be described as eq 18

$$\Delta H = \bar{\chi} \bar{\phi}_P \bar{\phi}_E \quad (18)$$

here $\bar{\phi}_P$ and $\bar{\phi}_E$ are the reduced volume fractions of thermoplastic polymer and epoxy prepolymer, respectively:

$$\bar{\phi}_P = \frac{\phi_P}{\phi_P + \phi_E} \quad (19)$$

Since the enthalpy of mixing is not changed when expressed in terms of the volume fractions of two components in the pseudobinary mixture, it can be rewritten as

$$\Delta H = \bar{\chi} \bar{\phi}_P \bar{\phi}_E = \bar{\chi} \phi_1 \phi_2 \quad (20)$$

where ϕ_1 and ϕ_2 are the volume fractions of the pseudo-

binary components, i.e.

$$\phi_1 = \frac{\phi_E + \phi_C}{\phi_P + \phi_E + \phi_C}$$

$$\phi_2 = \frac{\phi_P}{\phi_P + \phi_E + \phi_C} \quad (21)$$

Thus the free energy of mixing per lattice site for our model system can be written as eq 22. All parameters

$$\frac{\Delta G_M}{kT} = \left[\frac{\phi_1 \ln \phi_1}{z_1} + \frac{\phi_2 \ln \phi_2}{z_2} \right] + \chi' \phi_1 \phi_2 \quad (22)$$

involved in the above procedure are listed in Table 1. As previously discussed, z_1 may be related to the degree of cure up to ca. 0.65, i.e., $z_1 = (1 - (6/5)\alpha)^{-1}$ and z_2 is equal to 7.692. In calculation of z_1 and z_2 , the value of 5.2 (lu³) is used as the initial molar volume of epoxy-curing agent, $\bar{V}_{1,0}$.

Several years ago, Williams et al.²⁴⁻²⁷ explained the cure process of the mixture of epoxy resin and the CTBN rubber in terms of the Flory-Huggins mixing free energy of mixture (see eq 22). According to their interpretation, z_1 increases with the epoxy conversion while z_2 remains constant during the cure process. It is expected that as z_1 increases with the epoxy conversion, there is a decrease in the absolute value of the entropic contribution to the free energy of mixing. This entropy loss leads to the demixing of the thermoplastic phase when the epoxy conversion passes through a particular degree of cure. As a result the structure factor $S(q,t)$ increases with curing time.

Figure 9a shows a plot of eq 22 at $T = 400$ K and various compositions up to z_1 of 2.5, which corresponds to α of 0.5. When α (or z_1) increases, the absolute value of the entropic contribution to the free energy of mixing decreases. If α increases further, the shape of the free energy curve allows the choice of a pair of points at different two compositions with a common tangent leading to the same ordinate intersection. These conjugated points correspond to equilibrium compositions because the chemical potential of each component is the same in both phases. The locus of these conjugated points is the equilibrium or binodal curve. Also, in the same region the free energy curve shows a pair of inflection points. Their locus is the spinodal curve. Figure 9b is the phase diagram of temperature T vs the volume fraction of thermoplastic polymer, ϕ_2 , for various z_1 . Initially ($z_1 = 1.0$), the mixture (at $T = 400$ K in our model system) is random and homogeneous. As the curing proceeds, z_1 increases and then the mixture is phase separated into two phases (whether metastable or unstable) after a certain curing time elapses.

Figure 9c is the phase diagram of the degree of cure vs the volume fraction of thermoplastic polymer. The stable region (homogeneous solution) is located below the equilibrium curve. The unstable area is located above the spinodal curve and the metastable region lies between both curves. The critical composition, $(\phi_2)_c$, of our model system is equal to 0.33. As the initial homogeneous mixture is cured, the binodal will be reached at a critical degree of cure, α_{cp} . Once in the metastable region the droplets of thermoplastic polymer (or epoxy prepolymer) are formed, and then the composition of thermoplastic polymer in the matrix will decrease (or increase if epoxy rich domain are formed). Clearly the trajectory of the matrix composition will

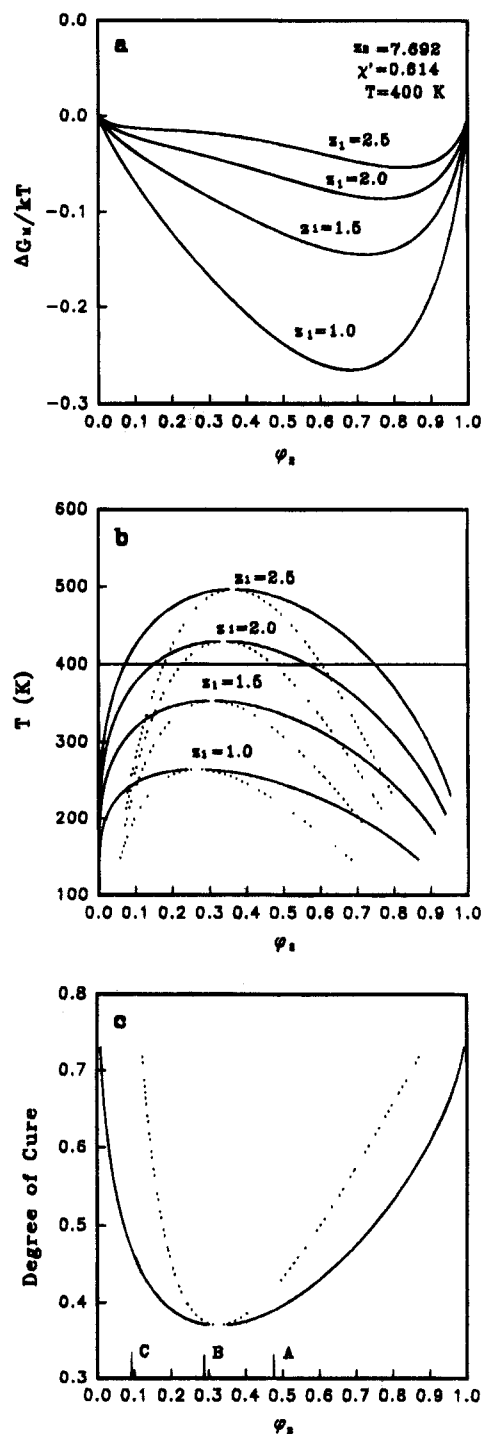


Figure 9. Thermodynamic interpretation of the simulation results: (a) free energy of mixing vs the volume fraction of thermoplastic polymer; (b) phase diagram of temperature T vs volume fraction; (c) phase diagram of degree of cure vs the volume fraction.

depend on the ratio of the intrinsic rate of phase separation to the rate of cure. If this ratio is large, i.e., phase separation proceeds much faster than cure, the trajectory will be close to the binodal curve. At a low value of the ratio, where the rate of cure is faster than phase separation, the trajectory will be vertical until spinodal decomposition takes place.

Figures 7 and 8 demonstrate the changes in the shape of scattering profiles at various cure conditions. The characteristic periodic distance is the hallmark of spinodal decomposition. This characteristic peak in scattering profiles suggests the development of a regularly phase separated structure, which is demonstrated as a

fact that the structure factor increases with the curing time. However, in the time evolution of the scattering patterns for the off-critical composition cured at lower reactivity, the scattering maxima are hardly observed during the entire time scale of the cure as shown in Figure 7a. At a given time, the structure factor monotonically decreases with increasing the magnitude of scattering vector, q , but the level of structure factor itself increases with the curing time. These are typical of the case where the phase separation occurs *via* the nucleation-growth mechanism. The homogeneous, sporadic nucleation and the growth of the domains results in the broad distribution of sizes of the dispersed domains, which results in the observed monotonically decreasing scattering profiles with the magnitude of scattering vector, q . Figure 7a shows that the homogeneous mixture separates into a two phase structure *via* nucleation-growth mechanism when the sample A is cured with a curing agent of reactivity of 10×10^{-3} . As seen in Figure 7b, however, the characteristic peak was observed when the system is cured with a curing agent of reactivity of 20×10^{-3} . It is noteworthy that the volume fraction of thermoplastic polymer of the sample A is higher than the critical composition, $(\phi_2)_i$. The structure factor of the system evolves through a metastable region when cured at reactivity of 10×10^{-3} , but the mixture separates into a two-phase structure *via* spinodal decomposition if cured at high rate of cure. If the rate of cure is too high, the system freezes in a homogeneous morphology, resulting in no development of the scattering pattern.

Figure 8 shows the characteristic peaks irrespective of reactivity, indicative of spinodal decomposition. The scattering profile of the fully cured resin has two peaks. The small angle peak can be assigned to the interdomain spacing between the large domains. The wide angle peak can be assigned to the overall spacing, including small domains.²⁸ During the cure, the small angle peak appears after a certain time lag and the wide angle peak appears at a fairly late stage. The interpretation on the basis of the Flory-Huggins theory explains why the spinodal decomposition is expected to take place in the curing process for the sample B. The sample B with reactivity of 2.0×10^{-3} (Figure 8a) and 5.0×10^{-3} (Figure 8b) show lower kinetic rate constants, $K = 0.74 \times 10^{-5} \text{ mcs}^{-1}$ and $K = 1.73 \times 10^{-5} \text{ mcs}^{-1}$ than the case ($K = 2.62 \times 10^{-5} \text{ mcs}^{-1}$) found in the sample A when cured at the reactivity of 10.0×10^{-3} . Although this system is cured more slowly than the case of Figure 7a, spinodal decomposition takes place for the system B, since the trajectory is vertical and the matrix composition passes nearly through the critical point. However, it is important to verify whether the observed periodicity is an artifact of underlying lattice or of the size of periodic box. This can be established by investigating the effect of lattice size on the peak position although it takes much longer computing time to simulate on the larger lattice size.

One can also estimate a periodic distance (Λ_m) of the phase-separated structure as a Bragg spacing from the peak scattering vector q_m of the scattering profile in Figure 8. The variation of Λ_m with curing time is shown in Figure 10 for various reactivities. The periodic distance slightly changes with curing time. According to the theory by Binder²⁹ and the interpretation of experimental finding by Inoue,³⁰ the periodic distance, Λ_m , is expected to decrease as the quench depth increases since the UCST-type phase boundary will be

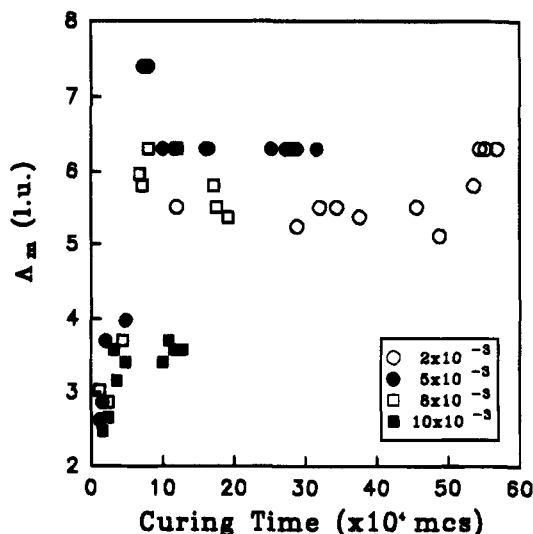


Figure 10. Time variation of periodic distance (Λ_m) with curing time for sample B.

elevated by the increase in the molecular weight of epoxy prepolymer with cure (Figure 9b). The higher quench depth takes the shorter periodic distance. When the effect of quench depth prevails over the coarsening process, the periodic distance may slightly decrease with curing time (for example, after ca. $7 \times 10^4 \text{ mcs}$, as seen in the Figure 10). Also, the periodic distance decreases with increasing reactivity. It can be seen that the mixture is gelled and loses mobility at an earlier stage of cure when cured at a higher reactivity.

Conclusions

This study has focused on the mechanism and behavior of phase separation during the cure process of epoxy resin in the mixture with thermoplastic polymer. A lattice model for simulating the cure process in the presence of thermoplastic polymer was developed. The cure behavior of a lattice model for the cure process of epoxy in the presence of thermoplastic polymer was investigated by assuming the second order reaction. The following conclusions were obtained: As the volume fraction of thermoplastic polymer increases, the apparent kinetic rate constant K decreases at the same reactivity. This may be interpreted as a diluent effect of added thermoplastic polymer. The gelation behavior is nearly consistent with the Flory-Stockmayer branching theory at a lower degree of cure. But a strong deviation from the theory at a higher degree of cure may be caused by the fact that the intramolecular reaction was neglected on the derivation of their theory. The time evolution of structure factor for various compositions of thermoplastic polymer could be interpreted in terms of the Flory-Huggins theory. Even though the phase separation behavior near the critical composition shows the spinodal decomposition irrespective of the magnitude of the reactivity, the phase separation mechanism at the off-critical composition is changed from nucleation-growth mechanism to spinodal decomposition as the cure rate increases.

References and Notes

- (1) Bucknall, C. B. *Toughened Plastics*; Applied Science Publishers Ltd.: London, 1977.
- (2) Riew, C. K.; Gillham, J. K. *Rubber-Modified Thermoset Resins*; American Chemical Society: Washington DC, 1984.
- (3) Baumgartner, A.; Binder, K. *J. Chem. Phys.* **1979**, *71*, 2541.

- (4) Kremer, K.; Binder, K.; Baumgartener, A. *J. Phys. A* **1982**, *15*, 2879.
- (5) Dial, M.; Crabb, K. S.; Crabb, C. C.; Kovac, J. *Macromolecules* **1985**, *18*, 2215.
- (6) Downey, J. P.; Crabb, C. C.; Kovac, J. *Macromolecules* **1986**, *19*, 2202.
- (7) Carmesin, I.; Kremer, K. *Macromolecules* **1988**, *21*, 2819.
- (8) Jo, W. H.; Ko, M. B. *Macromolecules* **1993**, *26*, 5473.
- (9) Deutsch, H. P.; Binder, K. *J. Chem. Phys.* **1991**, *94*, 2294.
- (10) Chakrabarti, A.; Toral, R.; Gunton, J. D.; Muthukumar, M. *J. Chem. Phys.* **1990**, *92*, 6899.
- (11) Glatter, O. In *Neutron, X-ray and Light Scattering; Introduction to an Investigative Tool for Colloidal and Polymeric Systems*; Linder, P., Zemb, Th., Eds.; North-Holland Delta Series: Paris, 1991; pp 38-39.
- (12) Horie, K.; Hiura, H.; Sawada, M.; Mita, I.; Kambe, H. *J. Polym. Sci.: A1* **1970**, *8*, 1357.
- (13) Sourour, S.; Kamal, M. R. *Thermochim. Acta* **1976**, *14*, 41.
- (14) Acitelli, M. A.; Prime, R. B.; Sacher, E. *Polymer* **1971**, *12*, 335.
- (15) Prime, R. B.; Sacher, E. *Polymer* **1972**, *13*, 455.
- (16) Prime, R. B. *Polym. Eng. Sci.* **1973**, *13*, 365.
- (17) Sariban, A.; Binder, K. *Macromolecules* **1991**, *24*, 578.
- (18) Hoshen, J.; Kopelman, R. *Phys. Rev. B* **1976**, *14*, 3438.
- (19) Dean, P. *Cambridge Philos. Soc., Proc.* **1963**, *59*, 397.
- (20) Stauffer, D.; Coniglio, A.; Adam, M. *Adv. Polym. Sci.* **1982**, *44*, 103.
- (21) Flory, P. J. *Principles of Polymer Chemistry*; Cornell University: Ithaca, 1953; Chapter IX.
- (22) Sariban, A.; Binder, K. *Macromolecules* **1988**, *21*, 711.
- (23) Sariban, A.; Binder, K. *J. Chem. Phys.* **1987**, *86*, 5859.
- (24) Williams, R. J. J.; Borrajo, J.; Addabo, H. E.; Rojas, A. J. In *Rubber-Modified Thermoset Resins*, *Adv. Chem. Ser., No. 208*; Riew, C. K., Gillham, J. K., Eds.; American Chemical Society: Washington DC, 1984; Chapter 13.
- (25) Vazquez, A.; Rojas, A. J.; Addabo, H. E.; Borrajo, J.; Williams, R. J. *J. Polymer* **1987**, *28*, 1156.
- (26) Borrajo, J.; Riccardi, C. C.; Moschiar, S. M.; Williams, R. J. J. In *Rubber Toughened Plastics*; Riew, C. K. Ed.; American Chemical Society: Washington DC, 1989; Chapter 14.
- (27) Moschiar, S. M.; Riccardi, C. C.; Williams, R. J. J.; Verchere, D.; Sautereau, H.; Pascault, J. P. *J. Appl. Polym. Sci.* **1991**, *42*, 717.
- (28) Yamanaka, K.; Takagi, Y.; Inoue, T. *Polymer* **1989**, *60*, 1839.
- (29) Binder, K. *J. Chem. Phys.* **1983**, *79*, 6387.
- (30) Yamanaka, K.; Inoue, T. *J. Mater. Sci.* **1990**, *25*, 241.